

Incorporating Low-Cost GNSS Receivers for Deformation Monitoring in High-Rise Buildings

Jayamanne JAYAMANNE^{1, *}, Panos PSIMOULIS¹, John OWEN¹, Nigel PENNA², and Chenyu XUE¹

¹ *University of Nottingham, Nottingham, United Kingdom (jayamanne.jayamanne@nottingham.ac.uk)*

² *Newcastle University, Newcastle, United Kingdom*

**corresponding author*

Abstract

Deformation monitoring of high-rise buildings is crucial for ensuring structural integrity and safety. Traditional methods including conventional surveying techniques, while effective, often involve high costs and operational challenges. This research explores the feasibility of utilizing low-cost Global Navigation Satellite System (GNSS) receivers in monitoring deformations of high-rise buildings. This study focuses on examining deformations of slow movement, such as that due to temperature and solar radiation, and dynamic movement such that due to wind load and seismic activities. A series of controlled experiments assess the performance of low-cost receivers compared to high-precision geodetic equipment, for static, slow-motion and dynamic motion. We analyse the GNSS data of the low-cost GNSS receivers and compare them against geodetic GNSS receiver and independent high-precision Robotic Total Station (RTS) data. The study focuses on the assessment of the performance of the u-blox F9P dual frequency low-cost GNSS receiver when connected with three different types of antenna; with Leica AS10, Tallysman TWI and u-blox patch antennas. The results of the study show the impact of the antenna type and the GNSS satellite constellation on the performance of the low-cost GNSS receiver. However, it is revealed that the low-cost GNSS receiver, even with a low-cost antenna and the appropriate GNSS satellite constellation, has significant potential in providing reliable and accurate GNSS measurements, suitable for a sustainable monitoring network for high-rise buildings.

Keywords: High-Rise Buildings, Deformation Monitoring, Low-Cost GNSS

Received: 8th December 2024. Revised: 24th February 2025. Accepted: 10th March 2025.

1 Introduction

High-rise structures are broadly designed and developed in the last decade around the globe, and they experience a wide range of deformations due to complex architectural design, height, and exposure to multiple varying loading conditions and other environmental influences (Yuan, 2021). The expected deformations cover a range of types and magnitudes, usually determined during the design and the construction stage to ensure the structural integrity and the safety of occupants (Yuan, 2021; Takabatake et al., 2019). It is also important to monitor and evaluate the structural and positional deformations of high-rise buildings after construction to assure continued control over the

stability of the structure and comfort of the occupants.

The recent developments of Global Navigation Satellite Systems (GNSS) technology, with the multi-GNSS satellite constellations, the high sampling-rate (up to 100 Hz) and the advancements of GNSS data processing have enhanced significantly the precision and accuracy for positioning and deformation monitoring applications (Moschas and Stiros, 2011; Msaewe et al., 2021). There have been recent studies where multi-GNSS concept has been applied in monitoring the response of major civil engineering infrastructure, such as bridges (Meng et al., 2018; Msaewe et al., 2021). In contrast to traditional manual observations, which require many on-site

visits and extensive data processing, the utilisation of GNSS technology enables engineers to efficiently monitor the deformations with minimal human effort (Shults et al., 2023; Reguzzoni et al., 2022).

Recently, there has been a significant increase in the availability of mass-market low-cost GNSS receivers capable of achieving sub-centimeter accuracy which was once believed to only be possible with geodetic-grade receivers (Xue et al., 2021). This ongoing transition is modifying the scope of navigation, surveying, and other research applications, hence broadening the accessibility of high-precision positioning to a wider community (Hamza et al., 2021). The low-cost receivers are compact, light-weight, capable of measuring dual frequency bands (L1/L2, L1/L5, etc.) and priced ten to twenty times lower than the geodetic-grade receivers. There have been recent studies revealing the capacity of low-cost GNSS receivers in monitoring dynamic motion (Xue et al., 2022), and a first attempt to monitor the response of a suspension bridge (Xue and Psimoulis, 2023). However, it is needed to conduct further experiments to analyse the performance of low-cost GNSS receivers in monitoring the holistic response of structures, from the very slow to more dynamic response, such as those of tall buildings.

In this study, we experimentally explore the capabilities of dual-frequency low-cost GNSS receivers in terms of accuracy, precision and sustainability in monitoring deformations present in tall buildings. More specifically, we assess the performance of low-cost GNSS receivers and antennas against fully geodetic GNSS receivers through a set of controlled experiments which assess the noise levels and performance of the receivers during static conditions, slow-motion conditions and dynamic motion conditions.

2 Performance Analysis Under Static Conditions

2.1 Experimental Setup

The experiment was carried out on the rooftop laboratory of the Nottingham Geospatial Institute, Nottingham, UK. Three types of GNSS antennas were tested: (i) Leica GS10 geodetic antenna, (ii) u-blox patch antenna, and (iii) Tallysman TWI antenna in conjunction with a geodetic receiver (Leica GS10) and a low-cost receiver (u-blox F9P) as rover stations. This setup was facilitated by a signal splitter, allowing simultaneous data

collection from both geodetic and low-cost receivers for each antenna type.

The base station receiver and antenna were kept constant throughout the experiment as a fully geodetic grade setup: Leica AR25.R4 antenna with a Leica GR10 receiver. Both the base station and the rover were set on two pillars with known coordinates and within a baseline length of 17.4 m. Figure 1 illustrates the experimental design incorporated in the test.

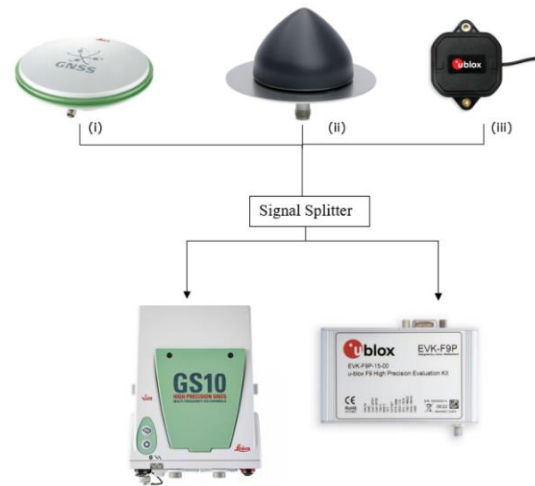


Figure 1: Experimental setup: (i) Leica AS10 Geodetic Antenna, (ii) Tallysman TWI Antenna and (iii) u-blox Patch Antenna connected through a signal splitter to a Leica GS10 Geodetic GNSS Receiver and u-blox F9P low-cost GNSS Receiver.

2.2 GNSS Data collection and Processing

Dual-frequency (L1/L2) GNSS data were collected with a sampling rate of 1 Hz over a continuous observation period of 24 hours. To ensure consistency in satellite constellations for GPS and Galileo, each test was conducted after 10 sidereal days from the previous. The data were processed using the RTKlib GNSS post-processing software with the following processing parameters:

Parameter	Value
Processing mode	Kinematic (PPK)
Elevation mask	7°
Filter Type	Combined
Ephemeris	Broadcast
Ionospheric Correction	Broadcast
Tropospheric Correction	Saastamoinen

RTKlib has been tested and applied on several similar studies (Xue et al., 2021; Xue et al., 2022), as it is suitable for Double-Difference GNSS solution providing with comprehensive tools for

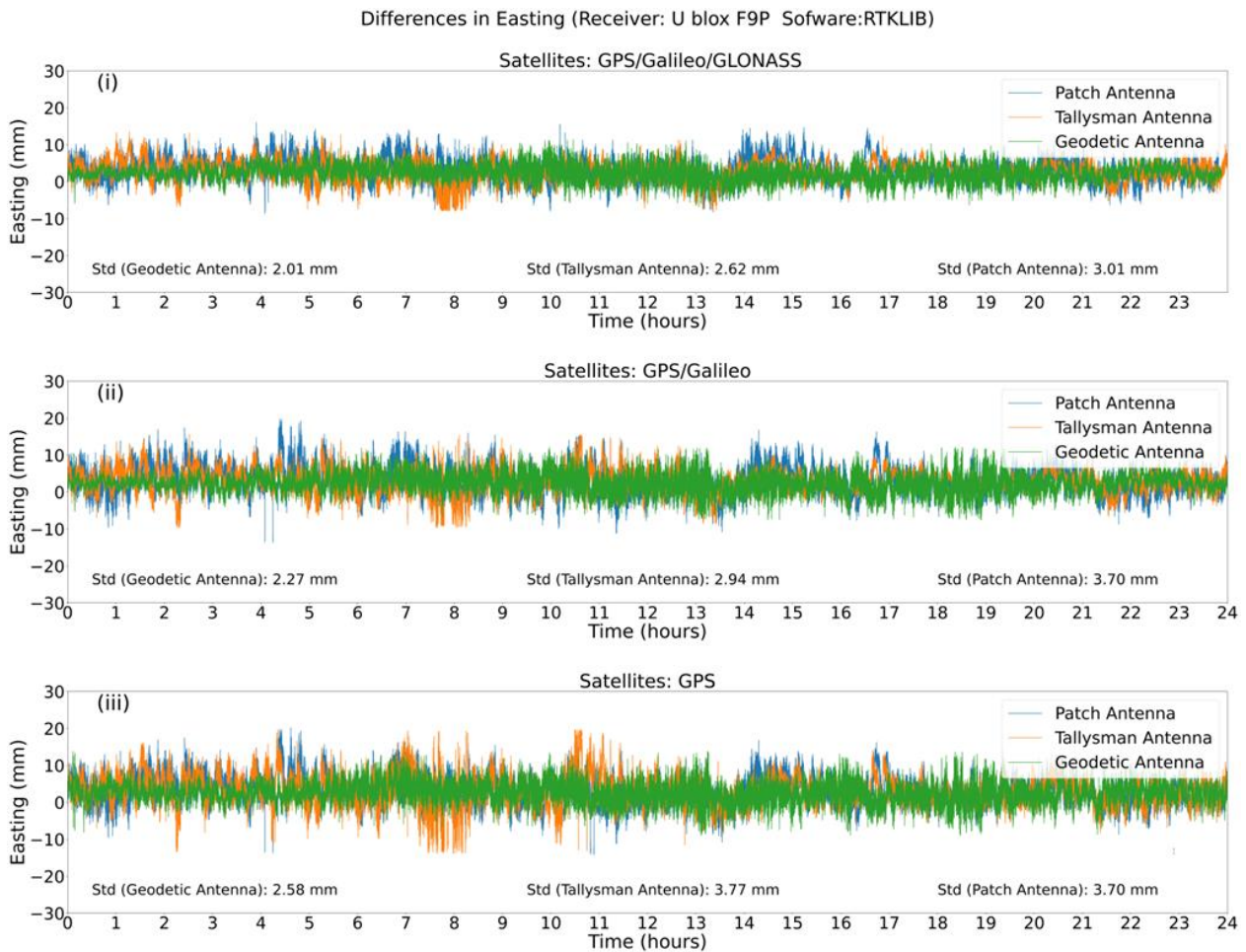


Figure 2: **Time Series of Easting Coordinate Residuals** - Difference between true and observed easting coordinates as recorded by the U-Blox F9P low-cost GNSS receiver using various antennas. Subplots: (i) GPS, Galileo and GLONASS, (ii) GPS and Galileo Only, (iii) GPS only.

analysing GNSS data including detailed examination of carrier phase and pseudo-range residuals, which has been tested and applied in several GNSS applications (Everett et al., 2022; Takasu and Yasuda, 2009).

2.3 Analysis and Results

The performance of the GNSS setups was analysed using their individual differences against the known British National Grid (BNG) coordinates of the rover station. The reference coordinates were obtained through a precise control survey conducted by geodetic grade GNSS receivers and Robotic Total Stations. Performances of the low-cost antenna-receiver combinations were analysed based on a GPS only, GPS and Galileo only, and a GPS, Galileo, and GLONASS solution.

All data were extensively checked for outliers using the 1.5 Interquartile Range (IQR) rule. The IQR, defined as the range between the first (Q1) and third quartiles (Q3), was used to establish the lower and upper bounds:

$$\text{Lower bound} = Q1 - 1.5 \times \text{IQR}$$

$$\text{Upper bound} = Q3 + 1.5 \times \text{IQR}$$

Any data point beyond these thresholds were classified as outliers and removed.

Figure 2 shows the time series of Easting coordinate differences as observed from the different antennas with a low-cost GNSS receiver. According to the plots, it is evident that the combined use of GPS, Galileo and GLONASS satellite systems significantly enhances the positional accuracy of all GNSS antennas used in the study.

Single-constellation systems, such as GPS only, tend to suffer from limited satellite geometry, particularly in areas where satellite visibility is restricted, leading to lower positional accuracy and precision (Jayamanne et al., 2019). Incorporating Galileo enhances the satellite coverage, improving the precision. However, adding GLONASS satellites further mitigates atmospheric errors and multipath effects (Chen et al., 2018; Xue et al., 2021).

This proves that multi-constellation systems leverage multiple satellite networks, thereby increasing the number of visible satellites, satellite geometry, and enhancing signal redundancy and reliability (Liu et al., 2019; Hamza et al., 2021; Xue et al., 2022). This precision enhancement is clearly evident during complex positioning tasks, as demonstrated in this experiment.

Among the antennas tested through this experiment, the u-blox patch antenna exhibits the lowest precision consistently, despite the satellite combination used. Patch antennas, commonly used for many low-cost geospatial applications, tend to have a lower resistance towards multipath errors and a poorer sensitivity than survey-grade GNSS antennas aligning with the findings from Xue et al., (2021) and Hamza et al., (2020). On the other hand, the Tallysman TWI antenna despite its low-cost depicts a comparable performance against the survey-grade antenna, due to the known antenna phase centre. Hence, this finding suggests that low-cost antennas of known phase centre can be used as a precise and sustainable alternative for geodetic applications.

In Table 1 is presented the standard deviation of the GNSS time series of both geodetic and low-cost GNSS receivers obtained using the three antennas and the three different GNSS satellite constellations.

Table 1: Comparison of antenna precision across GNSS configurations for geodetic receiver and low-cost receiver

Antenna	Satellites	Receiver	
		Geodetic Receiver	Low-Cost Receiver
Geodetic	GPS	2.4 mm	2.6 mm
	GPS/GAL	2.2 mm	2.3 mm
	GPS/GAL/GLO	1.8 mm	2.0 mm
Tallysman	GPS	3.4 mm	3.8 mm
	GPS/GAL	2.8 mm	2.9 mm
	GPS/GAL/GLO	2.4 mm	2.6 mm
Patch	GPS	3.2 mm	3.7 mm
	GPS/GAL	2.8 mm	3.7 mm
	GPS/GAL/GLO	2.4 mm	3.0 mm

The data shows only a minor decrease in precision when using a low-cost receiver. The geodetic antenna maintains comparable accuracy with the low-cost receiver, with minimal differences in

standard deviation, ranging from 0.04 mm to 0.53 mm. The Tallysman TWI antenna displays a modest increase in variation, with standard deviation differences between 0.75 mm and 3.6 mm. These small discrepancies in the precision highlight the capability of both low-cost antenna types to deliver precise results, even with low-cost receivers, even though the geodetic antenna leads to better results.

Based on the above-mentioned findings of the static test, subsequent experiments were designed to investigate the performance in slow and dynamic moving conditions.

3 Performance Analysis Under Slow Moving Conditions

3.1 Experimental Setup

The purpose of this experiment was to evaluate the performance of a low-cost GNSS system during gradual horizontal and vertical movements. Similar to the initial static observation test, three types of GNSS antennas—(i) Leica GS10 geodetic antenna, (ii) U-blox patch antenna and (iii) Tallysman TWI antenna—were tested with a low-cost receiver (u-blox F9P) and were used as the rover stations. The Leica GS10 geodetic antenna was connected via a signal splitter to a Geodetic Receiver (Leica GS10) to establish a full geodetic configuration.



Figure 3: Top- **Experimental setup** (i) Leica AS10 geodetic antenna connected to a Leica GS10 receiver and U-Blox F9P receiver, (ii) Tallysman TWI antenna and (iii) u-blox patch antenna connected to u-blox F9P receiver. Bottom-Movement simulation device incorporated for the test.

A movement simulation device was employed to manually simulate 1 cm horizontal and vertical displacements per hour. The 1 cm displacements were simulated to express slowly developed displacements with semi-static characteristics which are observed under low to moderate wind and/or daily temperature and solar-radiation variations. The horizontal movements were oriented along the East-West axis. 1 Hz dual frequency GNSS data were collected through-out the experiment. Reference data for the movements were collected through 1 Hz measurements using a Robotic Total Station (RTS; Psimoulis and Stiros, 2008, Takabatake et al., 2019).

3.2 Analysis and Results

Horizontal and vertical movements recorded by each GNSS set up were analysed and were compared against the reference movements from the RTS. For the horizontal movement simulations, the overall average precision of the full geodetic configuration was 1.56 mm. The Leica AS10 geodetic antenna, when paired with a low-cost receiver, demonstrated an average precision of 1.64 mm, indicating that geodetic antennas can be effectively combined with low-cost receivers to achieve remarkable performance. The combination of u-blox receiver with the Tallysman antenna

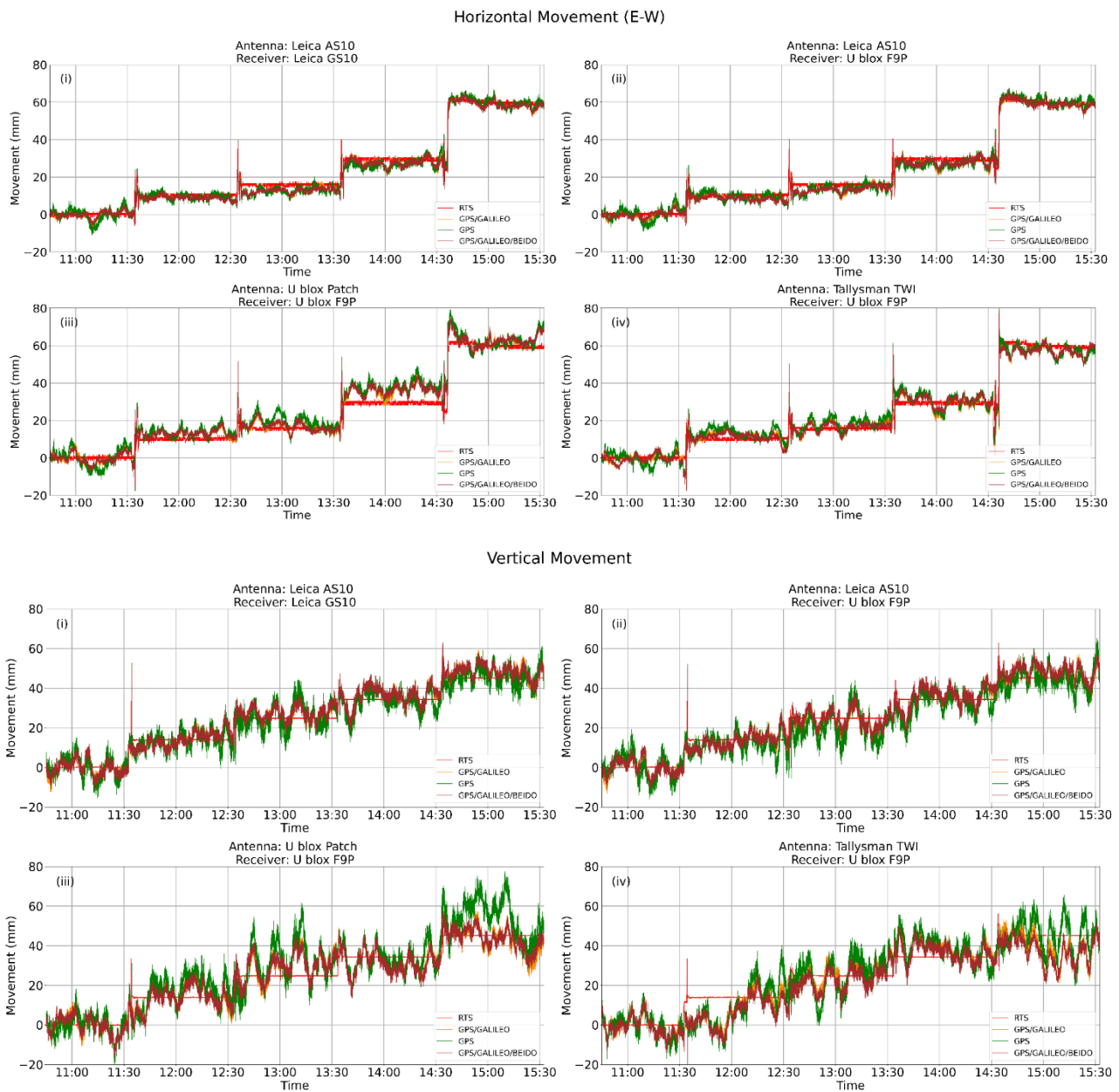


Figure 4: Horizontal and Vertical movements recorded by each GNSS setup- Subplots: (i) Leica AS10 geodetic antenna connected to a Leica GS10 geodetic receiver (ii) Leica AS10 geodetic antenna connected to a u-blox F9P low-cost receiver, (iii) u-blox patch antenna and (iv) Tallysman TWI antenna connected to u-blox F9P low-cost receiver.

exhibited a precision of 2.21 mm, indicating a degradation of 0.65 mm from the geodetic setup. The u-blox with patch antenna combination exhibited a precision of 2.43 mm, reflecting a decrease of 0.87 mm.

The noise during vertical movements is comparatively higher than the noise from horizontal movements in all configurations. However, the same trend was seen in terms of the precision of the data with the following standard deviations- Geodetic antenna with geodetic receiver: 3.64 mm, Geodetic antenna with low-cost receiver: 3.91 mm. Tallysman low-cost antenna with low-cost receiver: 4.72 mm, Patch low-cost antenna with low-cost receiver: 5.99 mm

The investigation of performance across the different antenna-receiver combinations provides the following ranking for each configuration. The Leica AS10 antenna, in conjunction with the GS10 receiver, displayed minimal noise as expected. The Leica AS10 antenna, with the u-blox receiver, exhibited performance closely akin to the first configuration. The Tallysman antenna, with the u-blox receiver, ranked next; however, it exhibited a considerable degree of noise. The patch antenna with the u-blox receiver exhibited the poorest performance, displaying the highest noise levels as illustrated in the Figures 4 and 5.

Incorporating multiple satellite systems has increased the performance across all antenna-receiver configurations by reducing the noise levels. The observed noise levels are also a result of multipath error impact (Xue et al., 2021). Consequently, the capability of each antenna in eliminating multipath errors is crucial to the overall performance of the system. The results clearly indicate the geodetic antenna is affected less by the multipath effect, while the Tallysman antenna, due to the modelled antenna phase centre, demonstrate better mitigation to the multipath effect with respect to the low-cost patch antenna.

The findings of this experiment prove that low-cost GNSS receivers can detect and monitor small slowly developed horizontal and vertical displacements. These results indicate their possible use in tracking the low-frequency shifts of the high-rise structures which are typically induced by factors such as solar radiation and minor wind forces.

4 Performance Analysis During Low-Frequency Dynamic Motion

4.1 Experimental Setup

The dynamic performance analysis was conducted based on computer-controlled vibrations of specific frequency range. The APS 113 shaker, a long-stroke, air-bearing electrodynamic shaker engineered for the accurate calibration and assessment of accelerometers and motion transducers, was used for the vibration experiments. The shaker has the capacity of force output up to 133 N and a peak-to-peak displacement of 158 mm, functioning within a frequency range of DC up to 200 Hz (Garg and Singh, 2021).

A Tallysman TWI antenna connected to a u-blox F9P receiver was placed on the shaker and sine waves of 0.1 Hz and 0.25 Hz were simulated to the shaker through a signal generator. The amplitudes of vibrations (i) below 1 cm (ii) around 2-3 cm, and (iii) around 6-7 cm were manually introduced. The simulated low-frequencies are prevalent to simulate the slow, long-period oscillations which are common for high rise buildings mainly due to wind load. The experimental vibration amplitude was determined based on mm-accuracy RTS measurements, which was used as the reference amplitude. The main objective of this test was to examine the performance of the low-cost GNSS receiver when combined with the low-cost Tallysman GNSS antenna, under dynamic motion conditions, where the challenges such as multipath noise are more complex and greater.



Figure 5: Left- The APS 113 shaker used for the experiment with Tallysman, Patch and Geodetic antennas. Right- U-blox F9P receivers connected to the antennas and Raspberry Pi devices to log the data.

4.2 Analysis and Results

The amplitudes recorded by the Tallysman antenna coupled with u-blox receiver were compared against the amplitudes recorded by the Robotic Total Station.

In Figures 6 and 7 is clearly demonstrated that the Tallysman antenna, paired with the low-cost

The higher error during larger amplitudes can be accounted due to noise amplification under dynamic conditions. However, further experimentation and data analysis is required to assess the performance of low-cost GNSS setups with different frequencies of vibrations and movement amplitudes.

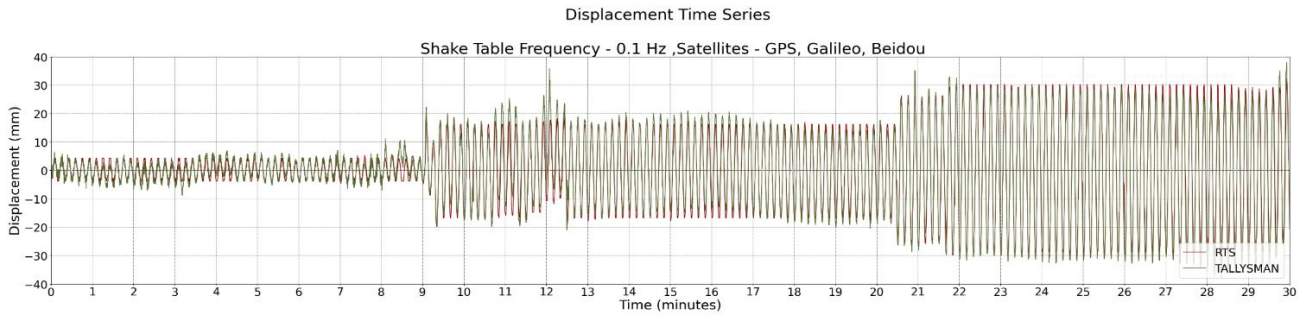


Figure 6: The displacements recorded by the Tallysman TWI antenna and RTS for 0.1 Hz.

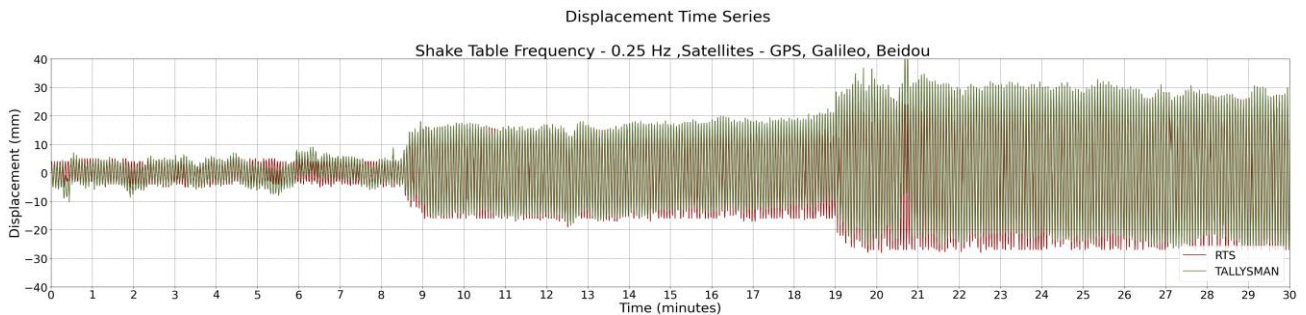


Figure 7: The displacements recorded by the Tallysman TWI antenna and RTS for 0.25 Hz.

receiver, has similar performance with RTS during low-frequency dynamic motions, in terms of the amplitude determination. The mean amplitude values of GNSS and RTS time-series were calculated as the mean value of the peak-amplitude of the vibration cycles of the GNSS and the RTS time-series. In Table 3 are presented the vibration amplitude as estimated by the RTS and GNSS time-series. It is obvious the relatively small error of the GNSS time-series, ranging between 1 and 2mm, with respect the RTS time-series.

Table 3: Mean Amplitude values recorded by Tallysman- u-blox GNSS setup and Robotic Total Station for 0.1Hz and 0.25Hz vibrations.

Frequency	Amplitude (mm)		Error (mm)
	RTS	Tallysman	
0.1 Hz	3.6	2.7	0.9
	15.9	15.3	0.6
	29.7	27.9	1.8
0.25 Hz	3.3	2.9	0.4
	13.9	13.6	0.3
	24.6	25.9	1.3

5 Conclusion and Recommendations

This research assessed the performance of low-cost GNSS receivers during static observations and both slow and dynamic displacement which can subsequently be utilized to detect equivalent movements in high-rise buildings. The results indicated that (i) a geodetic antenna paired with low-cost receivers can achieve performance comparable to a fully geodetic setup at a sub-millimeter level, and (ii) a low-cost GNSS antenna combined with low-cost GNSS receivers can attain sub-centimeter (< 5mm) precision through rigorous observation and processing techniques, such as the integration of multiple satellite constellations for observations. The results of this study are of accordance with similar studies that are conducted on applications of low-cost GNSS setup for deformation monitoring of flexible structures including tall buildings and long span bridges (Xue et al., 2022; Moschas and Stiros, 2011).

The subsequent phase of the research is to further investigate low-cost GNSS configurations in more static and dynamic motion scenarios. This phase will concentrate on case studies of high-rise buildings to assess the performance of these systems in long-term operational environments. This research seeks to enhance knowledge of the possible applications and limitations of low-cost GNSS technologies in real life situations by examining the advanced use cases.

Acknowledgements

This research is funded by the EPSRC, UK through the Center for Doctoral Training in Geospatial Systems, with the grant reference EP/S023577/1.

References

- Chen, Q., Jiang, W., Meng, X., Jiang, P., Wang, K., Xie, Y., and Ye, J. (2018). Vertical deformation monitoring of the suspension bridge tower using GNSS: A case study of the Forth Road Bridge in the UK. *Remote Sensing*, 10(3):364.
- Everett, T., Taylor, T., Lee, D.-K., and Akos, D. M. (2022). Optimizing the use of RTKLIB for smartphone-based GNSS measurements. *Sensors*, 22(10):3825.
- Garg, N. and Singh, M. (2021). Measurement uncertainty in primary calibration of accelerometer complex sensitivity at low frequencies. *MAPAN*, 36(4):821–831.
- Hamza, V., Stopar, B. and Sterle, O. (2021). Testing the performance of multi-frequency low-cost GNSS receivers and antennas. *Sensors*, 21(6):2029.
- Hamza, V., Stopar, B., Turk, G., and Sterle, O. (2020). Testing multi-frequency low-cost GNSS receivers for geodetic monitoring purposes. *Sensors*, 20(16):4375.
- Jayamanne, J., Perera, C., and Vandebona, R. (2019). Evaluating the applicability of open source GNSS post-processing software for applications of surveying.
- Liu, X., Guo, G., and Li, H. (2019). Study on damage of shallow foundation building caused by surface curvature deformation in coal mining area. *KSCE Journal of Civil Engineering*, 23:4601–4610.
- Meng, X., Nguyen, D. T., Xie, Y., Owen, J. S., Psimoulis, P., Ince, S., & Bhatia, P. (2018). Design and implementation of a new system for large bridge monitoring—GEOSHM. *Sensors*, 18(3), 775.
- Moschas, F. and Stiros, S. (2011). Measurement of the dynamic displacements and of the modal frequencies of a short-span pedestrian bridge using GPS and an accelerometer. *Engineering structures*, 33(1):10–17.
- Msaewe, H. A., Psimoulis, P. A., Hancock, C. M., Roberts, G. W., and Bonenberg, L. (2021). Monitoring the response of Severn Suspension Bridge in the United Kingdom using multi-GNSS measurements. *Structural Control and Health Monitoring*, 28(11): e2830.
- Psimoulis, P. A., & Stiros, S. C. (2008). Experimental assessment of the accuracy of GPS and RTS for the determination of the parameters of oscillation of major structures. *Computer-Aided Civil and Infrastructure Engineering*, 23(5), 389–403.
- Reguzzoni, M., Rossi, L., De Gaetani, C. I., Caldera, S., and Barzaghi, R. (2022). GNSS-based dam monitoring: The application of a statistical approach for time series analysis to a case study. *Applied Sciences*, 12(19):9981.
- Shults, R., Ormambekova, A., Medvedskij, Y., and Annenkov, A. (2023). GNSS-assisted low-cost vision-based observation system for deformation monitoring. *Applied Sciences*, 13(5):2813.
- Takabatake, H., Kitada, Y., Takewaki, I., and Kishida, A. (2019). *Simplified dynamic analysis of high-rise buildings*. Springer.
- Takasu, T. and Yasuda, A. (2009). Development of the low-cost RTK-GPS receiver with an open-source program package RTKLIB. In *International symposium on GPS/GNSS*, volume 1, pages 1–6. International Convention Center Jeju Korea Seogwiposi, Republic of Korea.
- Xue, C., Psimoulis, P., and Meng, X. (2022). Feasibility analysis of the performance of low-cost GNSS receivers in monitoring dynamic motion. *Measurement*, 202:111819.
- Xue, C., Psimoulis, P., Zhang, Q., and Meng, X. (2021). Analysis of the performance of closely spaced low-cost multi-GNSS receivers. *Applied Geomatics*, 13:415–435.
- Xue, C., & Psimoulis, P. A. (2023). Monitoring the dynamic response of a pedestrian bridge by using low-cost GNSS receivers. *Engineering Structures*, 284, 115993.
- Yigit, C. O., El-Mowafy, A., Anil Dindar, A., Bezcioglu, M., and Tiryakioglu, I. (2021). Investigating performance of high-rate GNSS-PPP and PPP-AR for structural health monitoring: Dynamic tests on shake table. *Journal of surveying engineering*, 147(1):05020011.
- Yuan, S. (2021). High-rise building deformation monitoring based on remote wireless sensor network. *IEEE Sensors Journal*, 21(22):25133–25141.